Lasers in Manufacturing Conference 2021

Contacting of cylindrical lithium-ion batteries using short pulse laser beam welding

Lukas Mayr[a*], Lazar Tomcic[a], Michael K. Kick[a], Christoph Wunderling[a], Michael F. Zaeh[a]

[a]*Institute for Machine Tools and Industrial Management, Technical University of Munich, Boltzmannstr. 15, 85748 Garching, Germany*

Abstract

The increasing demand for electric vehicles requires innovative manufacturing processes to reduce the production costs of energy storages while ensuring or improving the electrical performance. Laser beam welding (LBW) is a highly flexible and fast process for automated connecting of battery cells. A possibility to overcome the challenges in terms of copper welding, such as the high reflectivity and thermal conductivity, is the use of nanosecond laser pulses with peak powers up to several kilowatts. In this study, a pulsed laser welding process was found to achieve narrow weld seams with high aspect ratios and a low heat input. Despite the small joint areas, good electrical resistances and high tensile strengths could be obtained. By using tin-coated copper material, the joint strength as well as the process efficiency in terms of the possible feed rate were enhanced. Pulse shapes with longer pulse durations proved to require a lower feed rate due to system restrictions in terms of pulse frequencies.

Keywords: laser beam micro welding; nanosecond pulsed fiber laser; copper welding; electric mobility

1. Introduction and state of the art

In times of progressing electrification, the need for efficient joining processes for electrical contacts rises. In large battery storages, up to thousands of cells must be connected (Brand et al., 2015). Laser beam welding (LBW) is a contactless joining process that is suitable for this purpose because of its high degree of automation and precise energy input (Das et al., 2018). Hence, LBW has already been used in serial production for electronics and energy storage applications (Cai, 2017).

* Corresponding author. Tel.: +49 89 289 15569; fax: +49 89 289 15555.
E-mail address: lukas.mayr@iwb.tum.de.

Specific requirements for the contacting of cylindrical lithium-ion batteries (LIBs) were defined by Schmidt et al., 2016 and Schmitz et al., 2018. The joints have to withstand mechanical loads such as impacts and still provide low electrical resistances. Furthermore, a low heat input and avoidance of penetration of the cell housing have to be assured in order to prevent damages in the manufacturing process. Housings for cylindrical LIBs are often manufactured out of nickel-plated steel (DC04), also called hilumin®. For the cell connectors, highly electrically conductive materials like aluminum and copper are used (Schmidt et al., 2016). Especially copper is challenging for LBW due to its high reflectivity to near-infrared radiation.

To address this challenging task, several approaches using continuous wave (cw) or pulsed laser radiation were investigated. These include spatial power modulation of cw radiation in the near-infrared wavelength range, which allows an accurate adjustment of the process (Heinen et al., 2017). Additionally, green (Kaiser et al., 2015) or blue laser radiation (Britten et al., 2020) showed a positive effect on the LBW of copper, since the absorptivity is enhanced compared to near-infrared radiation.

Materials in the cell housing such as the separator and the electrolyte are thermally sensitive (Schmitz, 2019). Welding with pulsed laser radiation showed to be suitable because of the low heat input compared to cw-LBW (Mathivanan and Plapper, 2019). Temporal power modulation over the pulse duration achieved positive results for the contacting of cylindrical cells and for the LBW of copper components. A pulse modulation spot welding strategy including preheating, peak pulse and postheating (Dijken et al., 2003), was used for the contacting of homogeneous hilumin joints by Schmitz et al., 2018. Based on this pulse shape, spot LBW was successfully applied on joints of pure copper (Britten et al., 2016). An investigation of this pulse modulation strategy using green laser radiation was conducted by Kick et al., 2020. Therein, the welding with elongated pulse durations showed an increase in the mechanical joint strengths and a decrease of the electrical resistances.

Good mechanical and electrical properties can also be obtained using near-infrared laser pulses with peak powers in the kW range and repetition frequencies above 100 kHz. Haddad et al., 2020 joined pure copper (0.3 mm) to aluminum (0.4 mm) and bronze (0.3 mm) to DC04 (0.3 mm) using a pulsed beam source with 130 W maximum average emission power. Seven parallel lines were welded next to each other with a distance of 40 µm to enlarge the joint area. Thus, electrical resistances of around 287 µΩ for CuSn6 on DC04 and of 44 µΩ for Cu-ETP on Al99.5 and average joint strengths of 172 N/mm² and 80 N/mm², respectively, were determined. Other approaches to increase the joint area used a beam oscillation strategy for line welds and spirals for large spot welds, which were pursued by Ascari et al., 2020. Al99.5 (0.4 mm) was welded on nickel-plated copper (0.3 mm). The nickel-plating served to increase the absorptivity. In cross-sections, it was determined that an increase in the pulse emission frequency reduces the welding depth. In terms of the joint area, local maxima occur when varying the pulse frequency. Haddad et al., 2020 and Ascari et al., 2020 performed the welding with only one pulse shape with a specific pulse duration. In these two publications, longer pulses were not investigated although they are preferred for LBW processes according to Perveen et al., 2018.

2. Materials and methods

The beam source SP-200P-A-EP-Z-L-Y from SPI Lasers used in this study is similar to that of Ascari et al., 2020 and Haddad et al., 2020. This beam source can emit different waveforms, which have different specifications as exemplarily shown in table 1 and fig. 1. To determine the influence of different pulse durations t_P, three different waveforms (*WF*) were investigated experimentally. The welding results using waveform *WF0* with a t_P of 261 ns and a maximal energy per pulse E_P of 1.03 mJ were compared to *WF36* and *WF59* with 508 ns and 1.24 mJ and 1220 ns and 1.52 mJ, respectively. Since Ascari et al., 2020 determined that the weld seam depth decreases at higher frequencies, the waveform-specific pulse repetition frequency PRF_0

was set for every parameter set. The use of PRF_0 ensures the maximum pulse energy E_P for each waveform and, hence, maximum process efficiency in terms of the welding depth.

Focal spot positioning and beam shaping were performed by a SUPERSCAN IV-30-QU 2 D galvanometer scanning optics from RAYLASE GmbH in combination with a S4LFT2163 F-theta lens from Sill Optics GmbH & Co. KG. The welding set-up is shown in fig. 2a. Due to the Rayleigh length of around 500 µm, special attention has to be paid to an accurate positioning of the sample surface in the z-direction.

Table 1. Specifications of the laser welding set-up for the investigated waveforms

maximum laser power $P_{L,max}$		200 W	
maximum peak power P_P		10 kW	
emission wavelength λ		1060 nm	
beam quality M^2		1.3	
spot diameter d_f		31 µm	
Rayleigh length z_R		500 µm	
focal length f_r		163 mm	
waveform *WF*	*WF0*	*WF36*	*WF59*
maximum pulse energy E_P	1.03 mJ	1.24 mJ	1.52 mJ
pulse duration t_P	261 ns	508 ns	1220 ns
pulse repetition frequency PRF_0 [1]	200 kHz	166 kHz	135 kHz

[1] maximum pulse repetition frequency providing maximum pulse energy at rated power

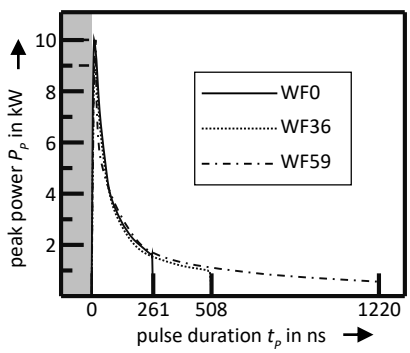

Fig. 1. Power curves of the investigated waveforms

With this set-up, two different copper materials were welded to the cell housing material hilumin. The use of Cu-ETP (electrolytic tough-pitch) with a tin-coating (Sn) was compared to the use of uncoated Cu-OF (oxygen-free) in order to investigate the influence of the higher absorptivity A of Sn. The Sn-coating is around 1 to 3 µm thick and has an absorptivity of around 20 % to radiation in the near-infrared wavelength range. The relevant physical properties of these materials are listed in table 2 showing a high similarity of Cu-OF and Cu(Sn). The copper thickness of around 0.3 mm was chosen for lower electrical losses in the connector, resulting in asymmetric overlap joints with the 0.2 mm thick hilumin.

Table 2. Physical properties of the used connector and cell housing materials at room temperature

description	*Cu-OF*	*Cu(Sn)*	*hilumin*
material	CW008A (Cu-OF), uncoated	CW004A (Cu-ETP, tin-plated)	hilumin® (nickel-plated stainless steel, DC04)
tensile strength R_m	260 MPa	255 – 315 MPa	270 – 690 MPa
melting temperature T_m	1084 K	1084 K	1809 K
thermal conductivity κ	391 W/(m·K)	394 W/(m·K)	52 W/(m·K)
electrical conductivity σ	58 m/(Ω·mm²)	58 m/(Ω·mm²)	10 m/(Ω·mm²)
absorptivity *A* (approx. 1060 nm)	6 %	20 % (Sn-layer)	30 %
thickness d_M	0.31 mm	0.30 mm	0.20 mm

For a first comparison, five linear weld seams were set in overlap joints according to fig. 2a and subsequently investigated in cross-sections. The time delay of Δt = 2 s between the processing of each line was chosen to reduce heat accumulation. High and unevenly distributed electrical resistances lead to energy loss and increased aging effects in assembled battery storages (Brand et al., 2015). Hence, the overlap joints were firstly

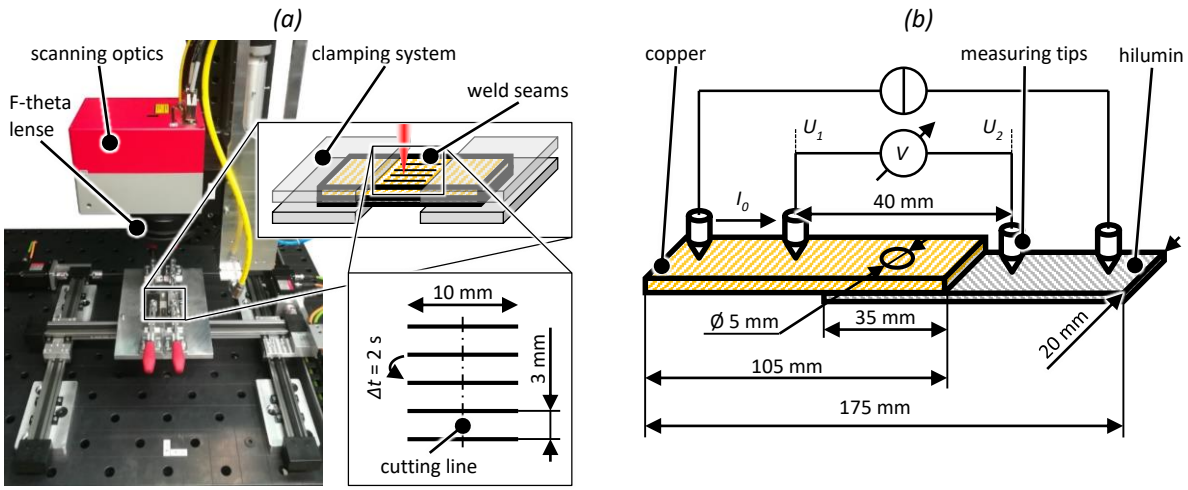

Fig. 2. *(a)* Short pulse laser welding set-up and the linear weld schematic for seam cross-sections and *(b)* the joint geometry as well as the set-up for electrical resistance measurement

tested in a four-point conductor measuring rig according tofig. 2b with a current of I_0 = 10 A. To evaluate the tensile joint strength F_m, these specimens were finally tested in a tensile shear test based on ISO 14273:2016. Circular weld seams with a diameter of 5 mm were welded to determine the electrical resistances and mechanical strengths.

Using these set-ups and the shown materials, experiments were conducted in order to investigate the welding process with nanosecond laser pulses for the contacting of cylindrical LIBs.

3. Parameter windows for welding of copper to hilumin

The parameters laser power P_L and feed rate v_L were varied while holding WF0 in order to find the process window for joining the metal sheets without fully penetrating the overlap. By that, the limits for full penetration of the copper materials and through the overlap joint could be obtained. In fig. 3a, it can be seen that the parameter window for the feed rate widens for both materials at higher average output powers. By that, not only the process efficiency can be increased but also small deviations in the feed rate might have less influence on the process outcome. On the one hand, no significant difference between both copper materials could be recognized apart from minor deviations for full penetration of the top sheet. On the other hand, the feed rate is constantly at least 10 % lower for Cu-OF than for Cu(Sn) required for full penetration of both sheets. This leads to the assumption, that the significantly higher absorptivity of Sn has only a minor influence on the provision of the necessary process energy. This could be due to the low melting temperature of about 500 K and the small thickness of 1 to 3 µm of the tin-coating, which is possibly melted and ablated by the first impinging pulses.

The cross-sections in fig. 3 (b – e) show welds with an increasing weld penetration depth and aspect ratios of up to 10:1. The high pulse peak powers in combination with the high emission frequencies lead to such rapid penetration into the materials that heat conduction only has a minor effect. This in return results in narrow weld seams. The burrs that occur even at the lower welding depth (see fig. 3b) indicate the highly dynamic welding process with high gas pressure, which leads to melt ejection.

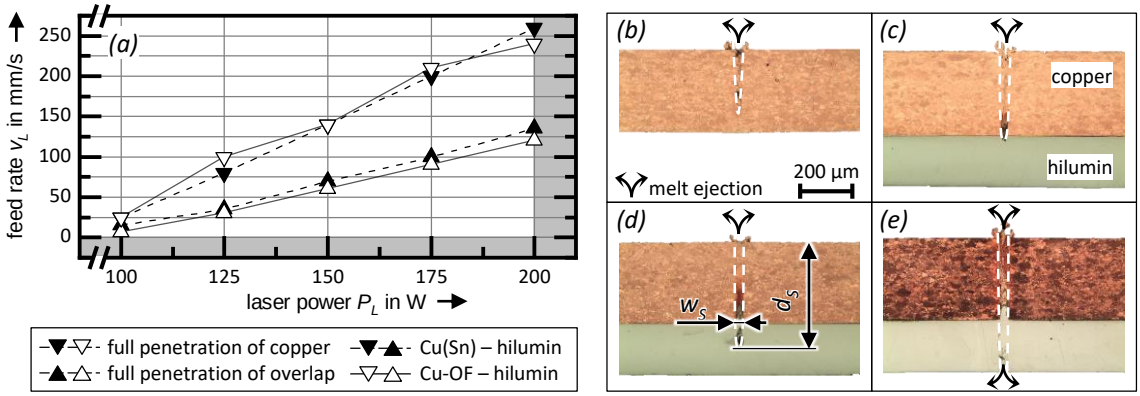

Fig. 3. *(a)* Parameter limits for full penetration of the upper sheet and the overlap in Cu(Sn)/Cu-OF – hilumin joints using WF0, *(b)* a weld seam not fully penetrating the copper and with melt ejection, *(c)* starting penetration of the hilumin, *(d)* a sufficiently deep weld seam with the measured seam geometry values (seam depth d_S and joint width w_S) and *(e)* full penetration of the overlap with melt ejection on both sides

4. Statistical analysis of the weld seam geometry

In order to quantify the parameter influence on the seam geometry, a design of experiments (DoE) according to table 3 was set up. The support points of the DoE for each material combination lie within the previously identified parameter window as shown infig. 4. Therein, parameter sets outside the process window were excluded using a D-optimal DoE. In total, 20 different parameter sets were investigated in a randomized order for each material combination.

Table 3. Parameter limits for the design of experiments (DoE)

parameter	support points	normalized support points
laser power P_L in W	[150.0; 162.5; 175.0; 187.5; 200.0]	[-1; -0.5; 0; 0.5; 1]
feed rate v_L in mm/s (for Cu-OF)	[75; 100; 125; 150; 175]	[-1; -0.5; 0; 0.5; 1]
feed rate v_L in mm/s (for Cu(Sn))	[100; 125; 150; 175; 200]	[-1; -0.5; 0; 0.5; 1]
waveform *WF*	[0; 36; 59]	[a; b; c]

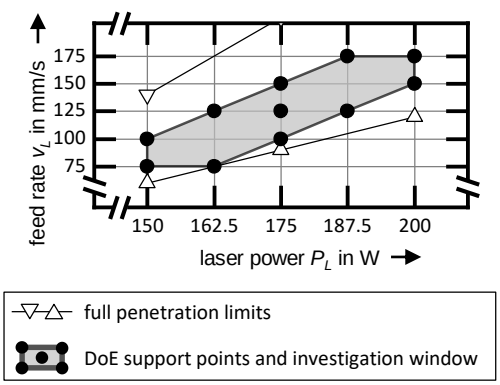

Fig. 4. Illustration of the DoE parameter support points in the parameter window exemplary for the Cu-OF – hilumin joints

The regression was performed using an analysis of variance. The regressed mean values of d_S in fig. 5a and of w_S in fig. 5b are plotted over the process parameters. A regression model with linear and interaction coefficients was used, which achieved coefficients of determination R^2 above 0.85 for all investigated factors. From the regression coefficients, it could be derived that the linear proportions of v_L and P_L as well as the interaction of P_L and WF show the highest influence on both the seam depth and the joint width. This results in approximately straight regression curves with only insignificant quadratic proportions as shown infig. 5.

According to the linear influence, d_S and w_S for both material combinations can be adjusted directly proportional with the laser power and inversely proportional with the feed rate.

With values for d_S under 300 µm, no connection in the overlap occured and, therefore, w_S was set to zero for the corresponding weld seam. Additionally, the joint widths tended to increase with higher seam depths, which resulted in a similar behavior of d_S and w_S for both material combinations. The comparison of Cu-OF and Cu(Sn) shows, that the tin-coating leads to deeper welds, which in return increases the values of w_S. The influence of the tin-coating hereby was significant, which stands in contrast to the smaller impact of the coating as shown infig. 3a.

The similar behavior of d_S and w_S also applied to the influence of the different waveforms. Shorter pulse durations or higher pulse frequencies led to higher seam depths. Therefore, the joint widths were also higher for WF0 than for WF36 and WF59. In contrast to Ascari et al., 2020, no frequencies above PRF0 were set. This would lead to a system-related decrease of the pulse energies and, hence, to lower values for d_S. Using WF59, a 50 % higher maximum pulse energy is emitted than with WF0. Therefore, it can be assumed that the 32.5 % lower set pulse frequency PRF_0 for WF59 in comparison with WF0 leads to significantly lower seam depths.

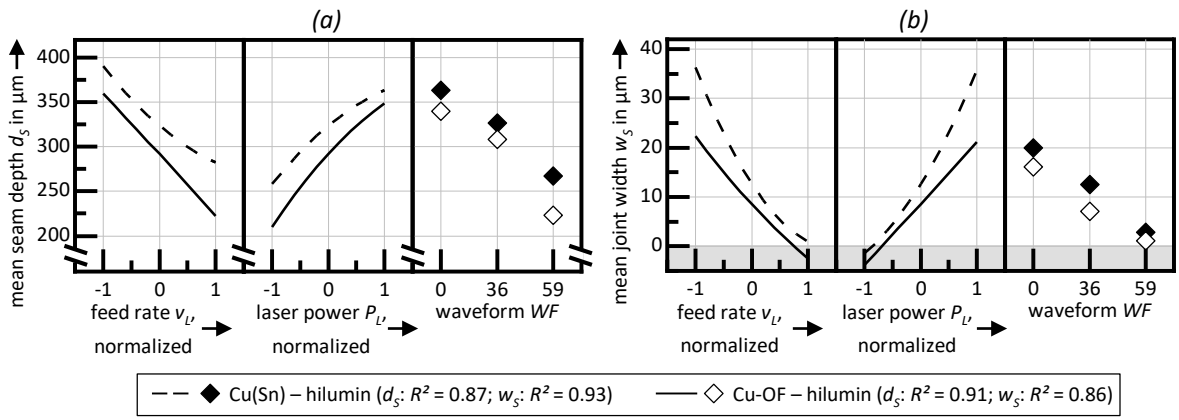

Fig. 5. Regression results from the analysis of the DoE with both material combinations for *(a)* the seam depth and *(b)* the joint width

For a high-quality interconnection of LIBs, the joint area and thus the joint width must be as wide as possible (Schmitz et al., 2018). Hence, the weld seams must be sufficiently deep to connect the metals, but not fully penetrate the housing. In order to reach these targeted process outcomes, the previously identified regression models were used to computationally approximate suitable parameter sets. This was done using the least-squares method. When the predicted values for d_S and w_S of a parameter set fully match with the process targets, an approximation fit with a value of 1 is achieved. The parameters with the best compliance for each material combination are listed in table 4 together with the resulting calculated and experimentally obtained values for d_S and w_S.

The approximations for both material combinations show high approximation fits which implies that this method results in suitable parameter sets. Applied on Cu(Sn), the approximation derived a parameter set including the maximum P_L of 200 W and WF36 with a higher feed rate v_L compared to Cu-OF. Using those parameters, the mean weld seam depth and joint width lie within the 95 % confidence interval for both material combinations. Moreover, the average seam depth from the experiments only differed around 4 % from the prediction and around 13 % in the joint width. Therefore, this parameter search method may be used for the tin-coated copper material. A restriction to this method is, that the d_S and the w_S fell below the lower confidence limit of 352.5 µm and 38.7 µm if the standard deviation is taken into account. In terms of the

uncoated Cu-OF, even the mean seam depth fell below the 95 % confidence limit of 378 µm. This resulted in a deviation from the regression of around three times compared to Cu(Sn) despite the high approximation fit.

Table 4. Approximated parameter sets with the corresponding regressed and experimentally obtained values for the seam depth and the joint width with standard deviations

	Cu(Sn) – hilumin		**Cu-OF – hilumin**	
approximated parameters	v_L = 123 mm/s, P_L = 200 W, WF36		v_L = 75 mm/s, P_L = 178 W, WF0	
approximation fit	0.95		0.99	
geometry value	seam depth d_S	joint width w_S	seam depth d_S	joint width w_S
predicted seam geometry in µm	400.0 ± 22.0	47.0 ± 3.8	415.5 ± 17.5	31.2 ± 3.2
95 % confidence interval in µm	352.5 – 447.5	38.7 – 55.3	378.0 – 453.0	24.4 – 38.1
95 % prediction interval in µm	332.6 – 467.4	35.2 – 58.8	355.4 – 475.6	20.2 – 42.3
measured seam geometry in µm	384.3 ± 56.5	40.7 ± 13.4	368.4 ± 84.7	19.3 ± 12.9
deviation experiment vs. prediction	4 %	13 %	12 %	38 %

5. Validation of approximated parameters through electrical and mechanical testing

The previously approximated parameter sets were used to determine the electrical joint resistance R_k and the ultimate tensile strength F_m of the copper hilumin joints. Five circular welds with a circle diameter of 5 mm were tested using tensile shear specimens and the results are listed in

	cu(sn) – hilumin	**cu-of – hilumin**
joint width w_s in µm	40.7 ± 13.4	19.3 ± 12.9
electrical resistance r_k in µω	728.5 ± 2.8	715.3 ± 9.7
breaking force f_m in n	450.8 ± 27.6	307.3 ± 35.6

. Electrical resistances R_k of slightly over 700 µΩ and breaking forces F_m of well over 250 N could be obtained for both materials.

Despite the significantly different joint widths, the contact resistances only differed slightly, whereas a 32 % higher joint strength occurred when using the tin-coated copper. Additional tests were conducted with Cu-OF in order to determine further optimization potential. On the one hand, a 10 % increased laser power and, on the other hand, a 10 % lower feed rate was investigated. Both parameter changes increased the joint strength by about 15 % which still falls below the value of Cu(Sn) with 450 N. Moreover, the increased energy input led to visible full penetration of the overlap joint, which might damage the materials within the battery housing.

Using this laser welding set-up, joint strengths of over 300 N were achieved despite the joint widths well below 60 µm. Additionally, intermetallic phases could be detected (see

figure 6. cross-section of a weld seam showing intermetallic phases, mechanical interlocking and a bridged joint gap (v_l = 75 mm/s, p_l = 162.5 w, wf36, cu-of – hilumin)

6. conclusion and summary

in this paper, the feasibility and parameter identification for the contacting of copper connectors and cylindrical lithium-ion batteries using a pulsed laser beam source were shown. based on the design of experiments, the influence of the process parameters laser power, feed rate and three different pulse durations on the resulting weld seam geometry was investigated. a change in the power and the feed showed an approximately linear effect on the welding depth. the investigated waveforms with higher pulse durations achieved lower weld seam depths, which could be compensated directly with a higher laser power, provided that the power limit of the system was not reached. the tin-coating on the copper material resulted in an increased energy input compared to the uncoated copper surface and, thus, in an enhanced process efficiency.

based on these results, a numerical parameter approximation was subsequently performed using the least-squares method. the optimized parameter sets were applied on circular welds which were tested electrically as well as mechanically. no significant difference in the electrical resistances but significantly higher tensile fracture forces up to over 450 n were determined using the tin-coated copper material.

this demonstrates the applicability of nanosecond laser pulses for the contacting of cylindrical lithium-ion batteries with coated and uncoated copper connectors. however, further investigations should be carried out with regard to the achievable mechanical strengths when strained with dynamic loads and accelerated aging. moreover, the determination of the weldability of different materials using pulsed laser beam sources can be advantageous in terms of the selection of suitable joining processes in various applications.

references

ascari, a., fortunato, a., dimatteo, v., 2020. short pulse laser welding of aluminum and copper alloys in dissimilar configuration. journal of laser applications 32 (2), #22025.

brand, m. j., schmidt, p. a., zaeh, m. f., jossen, a., 2105. welding techniques for battery cells and resulting electrical contact resistances. journal of energy storage 1 (2015), pp. 7–14.

britten, s. w., 2016, closing the gap between electronics and high power connectors: limbo. ltj 13 (2), pp. 53–55.

britten, s., schmid, l., molitor, t., ruetering, m., 2020. blue high-power laser sources for processing solutions in e-mobility and beyond. procedia cirp 94, pp. 592–595.

cai, w., 2017. lithium-ion battery manufacturing for electric vehicles: a contemporary overview. in: "*advances in battery manufacturing, services, and management systems*" li, j., zhou, s., han, y., editors. hoboken, new jersey: john wiley & sons (ieee press series on systems science and engineering). vol. 135, pp. 1–28.

das, a., li, d., williams, d., greenwood, d., 2018. joining technologies for automotive battery systems manufacturing. world electric vehicle journal 9 (2).

dijken, d. k.; hoving, w.; hosson, j. th. m. de, 2003. laser penetration spike welding: a microlaser welding technique enabling novel product designs and constructions. journal of laser applications 15 (1), pp. 11–18.

haddad, e., helm, j., olowinsky, a., gillner, a. 2020. nanosecond pulsed fiber laser as a tool for laser micro welding. procedia cirp 94, pp. 571–576.

heinen, p., haeusler, a., mehlmann, b., olowinsky, a., 2017. laser beam microwelding of lithium-ion battery cells with copper connectors for electrical connections in energy storage devices. lasers in engineering (2017) 36, pp. 147–167.

kaiser, e., huber, r., stolzenburg, c., killi, a., 2015. sputter-free and reproducible laser welding of electric or electronic copper contacts with a green laser. in "*lasers in manufacturing conference*" wlt e.v. editor. munich 2015.

kick, m., habedank, j. b., heilmeier, j., zaeh, m. f., 2020. contacting of 18650 lithium-ion batteries and copper bus bars using pulsed green laser radiation. procedia cirp 94, pp. 577–581.

mathivanan, k., plapper, p., 2019. laser welding of dissimilar copper and aluminum sheets by shaping the laser pulses. procedia manufacturing 36, pp. 154–162.

perveen, a., molardi, c., fornaini, c., 2018. applications of laser welding in dentistry: a state-of-the-art review. micromachines 9 (5). #209

schmidt, p. a., schmitz, p., zaeh, m. f., 2016. laser beam welding of electrical contacts for the application in stationary energy storage devices. journal of laser applications 28 (2016) 2, #22423.

schmitz, p., habedank, j. b., zaeh, m. f., 2018. spike laser welding for the electrical connection of cylindrical lithium-ion batteries. journal of laser applications 30 (2018) 2, #012004.) which could lead to brittle behavior of heterogeneous overlap joints. Therefore, the interconnection phenomena of this laser welding process have to be investigated in more detail.

Figure 6. Cross-section of a weld seam showing intermetallic phases, mechanical interlocking and a bridged joint gap (v_L = 75 mm/s, P_L = 162.5 W, WF36, Cu-OF – hilumin)

7. Conclusion and summary

In this paper, the feasibility and parameter identification for the contacting of copper connectors and cylindrical lithium-ion batteries using a pulsed laser beam source were shown. Based on the design of experiments, the influence of the process parameters laser power, feed rate and three different pulse durations on the resulting weld seam geometry was investigated. A change in the power and the feed showed an approximately linear effect on the welding depth. The investigated waveforms with higher pulse durations achieved lower weld seam depths, which could be compensated directly with a higher laser power, provided that the power limit of the system was not reached. The tin-coating on the copper material resulted in an increased energy input compared to the uncoated copper surface and, thus, in an enhanced process efficiency.

Based on these results, a numerical parameter approximation was subsequently performed using the least-squares method. The optimized parameter sets were applied on circular welds which were tested electrically as well as mechanically. No significant difference in the electrical resistances but significantly higher tensile fracture forces up to over 450 N were determined using the tin-coated copper material.

This demonstrates the applicability of nanosecond laser pulses for the contacting of cylindrical lithium-ion batteries with coated and uncoated copper connectors. However, further investigations should be carried out with regard to the achievable mechanical strengths when strained with dynamic loads and accelerated aging. Moreover, the determination of the weldability of different materials using pulsed laser beam sources can be advantageous in terms of the selection of suitable joining processes in various applications.

References

Ascari, A., Fortunato, A., Dimatteo, V., 2020. Short pulse laser welding of aluminum and copper alloys in dissimilar configuration. Journal of Laser Applications 32 (2), #22025.

Brand, M. J., Schmidt, P. A., Zaeh, M. F., Jossen, A., 2105. Welding techniques for battery cells and resulting electrical contact resistances. Journal of Energy Storage 1 (2015), pp. 7–14.

Britten, S. W., 2016, Closing the Gap between Electronics and High Power Connectors: LIMBO. LTJ 13 (2), pp. 53–55.

Britten, S., Schmid, L., Molitor, T., Ruetering, M., 2020. Blue high-power laser sources for processing solutions in e-mobility and beyond. Procedia CIRP 94, pp. 592–595.

Cai, W., 2017. Lithium-Ion Battery Manufacturing for Electric Vehicles: a Contemporary Overview. in: "*Advances in battery manufacturing, services, and management systems*" Li, J., Zhou, S., Han, Y., Editors. Hoboken, New Jersey: John Wiley & Sons (IEEE Press series on systems science and engineering). Vol. 135, pp. 1–28.

Das, A., Li, D., Williams, D., Greenwood, D., 2018. Joining Technologies for Automotive Battery Systems Manufacturing. World Electric Vehicle Journal 9 (2).

Dijken, D. K.; Hoving, W.; Hosson, J. Th. M. de, 2003. Laser penetration spike welding: A microlaser welding technique enabling novel product designs and constructions. Journal of Laser Applications 15 (1), pp. 11–18.

Haddad, E., Helm, J., Olowinsky, A., Gillner, A. 2020. Nanosecond pulsed fiber laser as a tool for laser micro welding. Procedia CIRP 94, pp. 571–576.

Heinen, P., Haeusler, A., Mehlmann, B., Olowinsky, A., 2017. Laser Beam Microwelding of Lithium-ion Battery Cells with Copper Connectors for Electrical Connections in Energy Storage Devices. Lasers in Engineering (2017) 36, pp. 147–167.

Kaiser, E., Huber, R., Stolzenburg, C., Killi, A., 2015. Sputter-free and reproducible laser welding of electric or electronic copper contacts with a green laser. in "*Lasers in Manufacturing Conference*" WLT e.V. Editor. Munich 2015.

Kick, M., Habedank, J. B., Heilmeier, J., Zaeh, M. F., 2020. Contacting of 18650 lithium-ion batteries and copper bus bars using pulsed green laser radiation. Procedia CIRP 94, pp. 577–581.

Mathivanan, K., Plapper, P., 2019. Laser welding of dissimilar copper and aluminum sheets by shaping the laser pulses. Procedia Manufacturing 36, pp. 154–162.

Perveen, A., Molardi, C., Fornaini, C., 2018. Applications of Laser Welding in Dentistry: A State-of-the-Art Review. Micromachines 9 (5). #209

Schmidt, P. A., Schmitz, P., Zaeh, M. F., 2016. Laser beam welding of electrical contacts for the application in stationary energy storage devices. Journal of Laser Applications 28 (2016) 2, #22423.

Schmitz, P., Habedank, J. B., Zaeh, M. F., 2018. Spike laser welding for the electrical connection of cylindrical lithium-ion batteries. Journal of Laser Applications 30 (2018) 2, #012004. also shows the possibility to perform joint gap bridging of at least 10 µm if sufficiently high process energy is provided.

Table 5. Electrical resistance and tensile joint strength with standard deviation obtained from welding experiments using the approximated parameter sets

	Cu(Sn) – hilumin	**Cu-OF – hilumin**
joint width w_S in µm	40.7 ± 13.4	19.3 ± 12.9
electrical resistance R_k in µΩ	728.5 ± 2.8	715.3 ± 9.7
breaking force F_m in N	450.8 ± 27.6	307.3 ± 35.6

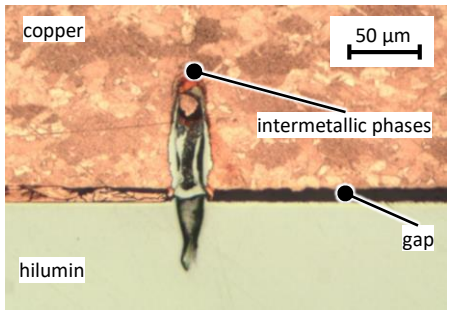

Figure 6. Cross-section of a weld seam showing intermetallic phases, mechanical interlocking and a bridged joint gap (v_L = 75 mm/s, P_L = 162.5 W, WF36, Cu-OF – hilumin)

8. Conclusion and summary

In this paper, the feasibility and parameter identification for the contacting of copper connectors and cylindrical lithium-ion batteries using a pulsed laser beam source were shown. Based on the design of experiments, the influence of the process parameters laser power, feed rate and three different pulse durations on the resulting weld seam geometry was investigated. A change in the power and the feed showed an approximately linear effect on the welding depth. The investigated waveforms with higher pulse durations achieved lower weld seam depths, which could be compensated directly with a higher laser power, provided that the power limit of the system was not reached. The tin-coating on the copper material resulted in an increased energy input compared to the uncoated copper surface and, thus, in an enhanced process efficiency.

Based on these results, a numerical parameter approximation was subsequently performed using the least-squares method. The optimized parameter sets were applied on circular welds which were tested electrically as well as mechanically. No significant difference in the electrical resistances but significantly higher tensile fracture forces up to over 450 N were determined using the tin-coated copper material.

This demonstrates the applicability of nanosecond laser pulses for the contacting of cylindrical lithium-ion batteries with coated and uncoated copper connectors. However, further investigations should be carried out with regard to the achievable mechanical strengths when strained with dynamic loads and accelerated aging. Moreover, the determination of the weldability of different materials using pulsed laser beam sources can be advantageous in terms of the selection of suitable joining processes in various applications.

References

Ascari, A., Fortunato, A., Dimatteo, V., 2020. Short pulse laser welding of aluminum and copper alloys in dissimilar configuration. Journal of Laser Applications 32 (2), #22025.

Brand, M. J., Schmidt, P. A., Zaeh, M. F., Jossen, A., 2105. Welding techniques for battery cells and resulting electrical contact resistances. Journal of Energy Storage 1 (2015), pp. 7–14.

Britten, S. W., 2016, Closing the Gap between Electronics and High Power Connectors: LIMBO. LTJ 13 (2), pp. 53–55.

Britten, S., Schmid, L., Molitor, T., Ruetering, M., 2020. Blue high-power laser sources for processing solutions in e-mobility and beyond. Procedia CIRP 94, pp. 592–595.

Cai, W., 2017. Lithium-Ion Battery Manufacturing for Electric Vehicles: a Contemporary Overview. in: "*Advances in battery manufacturing, services, and management systems*" Li, J., Zhou, S., Han, Y., Editors. Hoboken, New Jersey: John Wiley & Sons (IEEE Press series on systems science and engineering). Vol. 135, pp. 1–28.

Das, A., Li, D., Williams, D., Greenwood, D., 2018. Joining Technologies for Automotive Battery Systems Manufacturing. World Electric Vehicle Journal 9 (2).

Dijken, D. K.; Hoving, W.; Hosson, J. Th. M. de, 2003. Laser penetration spike welding: A microlaser welding technique enabling novel product designs and constructions. Journal of Laser Applications 15 (1), pp. 11–18.

Haddad, E., Helm, J., Olowinsky, A., Gillner, A. 2020. Nanosecond pulsed fiber laser as a tool for laser micro welding. Procedia CIRP 94, pp. 571–576.

Heinen, P., Haeusler, A., Mehlmann, B., Olowinsky, A., 2017. Laser Beam Microwelding of Lithium-ion Battery Cells with Copper Connectors for Electrical Connections in Energy Storage Devices. Lasers in Engineering (2017) 36, pp. 147–167.

Kaiser, E., Huber, R., Stolzenburg, C., Killi, A., 2015. Sputter-free and reproducible laser welding of electric or electronic copper contacts with a green laser. in "*Lasers in Manufacturing Conference*" WLT e.V. Editor. Munich 2015.

Kick, M., Habedank, J. B., Heilmeier, J., Zaeh, M. F., 2020. Contacting of 18650 lithium-ion batteries and copper bus bars using pulsed green laser radiation. Procedia CIRP 94, pp. 577–581.

Mathivanan, K., Plapper, P., 2019. Laser welding of dissimilar copper and aluminum sheets by shaping the laser pulses. Procedia Manufacturing 36, pp. 154–162.

Perveen, A., Molardi, C., Fornaini, C., 2018. Applications of Laser Welding in Dentistry: A State-of-the-Art Review. Micromachines 9 (5). #209

Schmidt, P. A., Schmitz, P., Zaeh, M. F., 2016. Laser beam welding of electrical contacts for the application in stationary energy storage devices. Journal of Laser Applications 28 (2016) 2, #22423.

Schmitz, P., Habedank, J. B., Zaeh, M. F., 2018. Spike laser welding for the electrical connection of cylindrical lithium-ion batteries. Journal of Laser Applications 30 (2018) 2, #012004.

Figure 7. Cross-section of a weld seam showing intermetallic phases, mechanical interlocking and a bridged joint gap (v_L = 75 mm/s, P_L = 162.5 W, WF36, Cu-OF – hilumin)